JOC The Journal of Organic Chemistry

pubs.acs.org/joc Note

DFT Study of Mechanism and Stereochemistry of Nickel-Catalyzed *trans*-Arylative Desymmetrizing Cyclization of Alkyne-Tethered Malononitriles

Yu-Qing Zheng, Chen-Long Li, Wen-Bo Liu,* and Zhi-Xiang Yu*

Cite This: *J. Org. Chem.* 2022, 87, 16079−16083 Read Online

ACCESS | Metrics & More | Article Recommendations | Supporting Information

ABSTRACT: Present here is a density functional theory (DFT) study of the mechanism and origin of enantioselectivity of Ni-catalyzed desymmetric cyclization of alkyne-tethered malononitriles and aryl boronic acids. The reaction starts from transmetalation and arylnickel addition, followed by *trans* to *cis* isomerization to give *cis*-alkenyl nickel species. The stereodetermining step is the CN insertion, which prefers a transition state with the bystander CN group staying away from the ligand to reduce steric repulsion, and gives the final (*R*)-product.

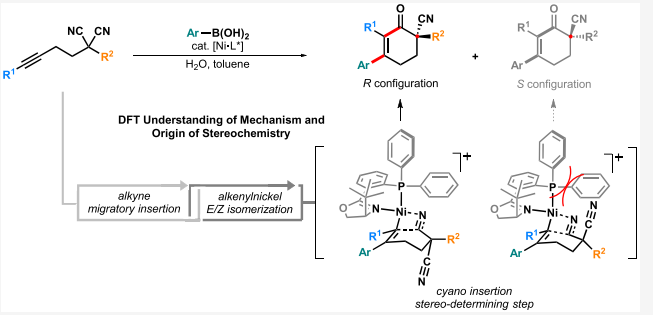

Developing new methods to access all-carbon quaternary stereocenters, which are widely found in natural products and pharmaceuticals,[1] is still a research frontier in organic chemistry, even though many advances have been achieved. To further push this frontier forward, understanding the mechanisms of these reactions and finding guiding rules as well as principles for reaction design are important.[2] Recently, we developed an intramolecular desymmetrizing cascade annulation reaction of prochiral alkyne-tethered malononitriles and aryl boronic acids to construct cyano-containing all-carbon quaternary centers.[3] This malononitrile desymmetrizing strategy provides an efficient and unique means to access functional group-enriched quaternary carbon units, enabling downstream diverse transformations (Scheme 1). The advantage of this strategy was further demonstrated through amino- or oxy-palladation/cyano addition,[4] [2 + 2 + 2] cyclization,[5] and reductive aryl/alkenyl−cyano cyclization couplings[6] to construct enantioenriched carbazolones, isocoumarins, pyridines, and indanones, respectively.

Scheme 1. Nickel-Catalyzed Desymmetrizing Annulation of Alkyne-Tethered Malononitriles with Aryl Boronic Acids

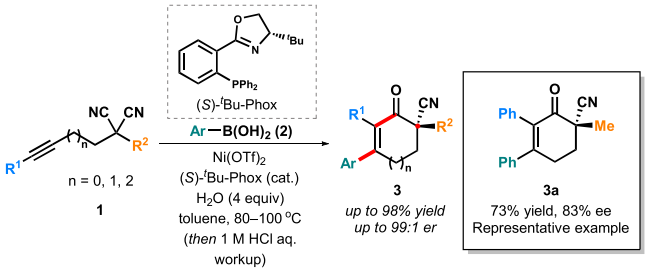

Based on the literature precedent, we proposed the mechanism for this reaction, using **1a** as an example (Scheme 2). Initially, water-assisted transmetalation between phenyl boronic acid **2a** and the nickel catalyst **I** generates an arylnickel species.[7,8] Then the alkyne moiety of **1a** coordinates to the arylnickel species, delivering intermediate **II**. After that, migratory insertion of the triple bond of the alkyne into the Ni−C bond gives rise to a key intermediate, *Z*-alkenylnickel species **III**. Then isomerization of the *Z*-alkenylnickel[9−11] produces the corresponding *E*-alkenylnickel species **IV**, which is capable of the intramolecular CN insertion to cycloheximidylnickel **V**. Further protonation of **V** provides the imine product **VI** and regenerates the catalyst for the next catalytic cycle. In the present paper, we report our DFT studies of the mechanism and the origin of the selectivity of this reaction, which are important to understand this reaction as well as related ones for further reaction optimization and design of new reactions or catalysts in the future.

The model reaction of DFT investigations is given in Figure 1.[12,13] In the target reaction, alkyne-tethered disubstituted malononitrile **1a** was treated by 2 equiv of phenyl boronic acid **2a** under the optimal conditions: 10 mol % of $Ni(OTf)_2$, 12

Received: May 28, 2022
Published: November 16, 2022

Scheme 2. Proposed Catalytic Cycle

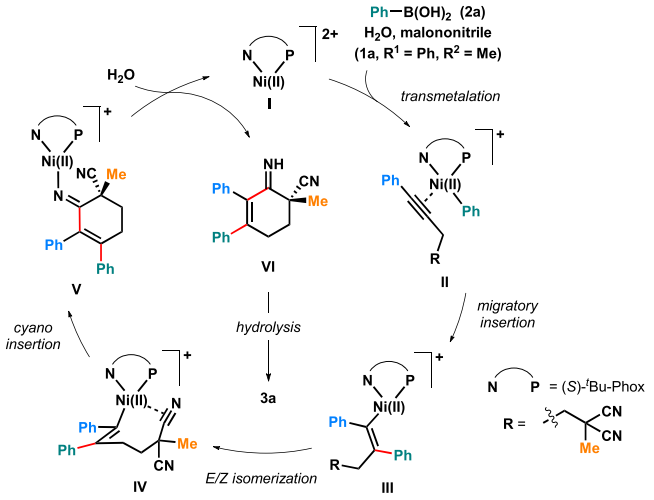

mol % of (*S*)-^{t}Bu-Phox ligand, and 4 equiv of water in toluene at 80 °C. Experimentally, this reaction gave the product **3a** in 73% yield with 83% ee. The valence state of the nickel catalyst remains unchanged during the process since no redox additives or redox steps (e.g., oxidative addition or reductive elimination) were involved. In what follows, we describe the overall pathways step by step.

Previous studies of Suzuki−Miyaura cross-coupling found that four-coordinated "ate" species are necessary for the process through "boronate" or "oxo-metal" pathways.[7a] Considering the recently detailed computational investigation of boron-to-nickel transmetalation by Perego, Ciofini, and Grimaud,[7b] as well as the vital role of water in our experiments, we suggested that the nickel complex **I** combines with an aryl boronate first to give **INT1** as the catalytic species, where the phenyl group in the boronic acid coordinates to the Ni center.[14] This is followed by a transmetalation process via a four-membered ring transition state, in which an aryl group is transferred to the metal center, with a low free energy barrier of 5.2 kcal/mol. The resulting **INT2** then undergoes a ligand exchange reaction with **1a** to form intermediate **INT3**, releasing a boric acid. Formation of **INT3** is exergonic by 19.3 kcal/mol from **INT2**, in which one of the CN groups in the substrate coordinates to the Ni atom.

After that, reorganization of the coordination mode in **INT3** leads to two complexes, **INT4** and **INT4′**. The energy barrier of direct cyano insertion from **INT3** is 26.2 kcal/mol (see **TS3**, blue line in Figure 1), which is disfavored compared to the competing pathway discussed below and is consequently ruled out for further investigation. Notably, **INT4**, in which an alkyne is situated on the opposite site of the phosphorus atom, is 1.7 kcal/mol more stable than **INT4′**, in which an alkyne lies on the opposite of the nitrogen atom. This can be understood by the *trans* effect of phosphine,[15] because phosphine is a strong σ donor and can increase the electron density of the central metal, which consequently strengthens the π-back bonding of metal to the alkyne at the *trans* position of phosphine.

In principle, both **INT4** and **INT4′** can undergo the followed steps in the catalytic cycle to give the final product. However, the process from **INT4** to the final product is kinetically favored. Alkyne insertion takes place via **TS4**, giving rise to **INT5**. This step requires an activation free energy of 0.4 kcal/mol and is exergonic by 20.5 kcal/mol. On the other hand, **INT4′** can undergo alkyne insertion via **TS4′**. But the Gibbs free energy of **TS4′** is higher than that of **TS4** by 10.5 kcal/mol. Therefore, the pathway via **INT4′** and **TS4′** is not favored. We also investigated the followed steps in this disfavored pathway to better understand this selectivity (the orange line of Figure 1), which will be discussed later on in this paper.

The alkenylnickel species **INT5**, with the alkyl chain and the nickel standing on different sides of the alkene, is geometrically infeasible to undergo CN insertion. Therefore, a *trans* to *cis* isomerization for **INT5** is demanded. We can locate such an isomerization transition state, **TS5**, according to a flexible "scan" calculation by varying the Ni−C1−C2−C3 dihedral angle (Figure 2). Such a rotation was proposed by Huggins and Bergman,[9] and was further explored by Wilger,[10] Werz,[11] Cho,[13c] and Chang[13d] recently. In the present reaction, this process requires an activation free energy of 19.1 kcal/mol, indicating that the *Z*/*E* isomerization process is feasible under the experimental conditions. Formation of *trans*-adduct alkenylnickel species **INT6** from *cis*-adduct species **INT5** is

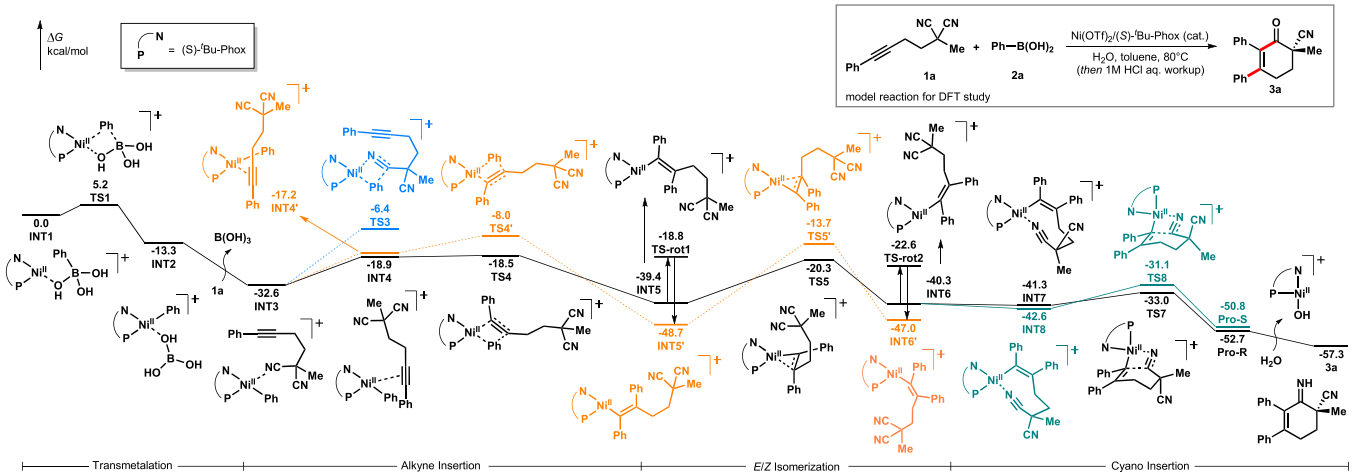

Figure 1. Relative Gibbs free energy profiles for regio- and enantioselective nickel-catalyzed alkyne addition/desymmetrizing cyclization cascade reaction of malononitrile derivatives at the B3LYP-D3(BJ)/def2-TZVP//SMD$_{toluene}$//B3LYP-D3(BJ)/def2-SVP level.

https://doi.org/10.1021/acs.joc.2c01269
J. Org. Chem. 2022, 87, 16079−16083

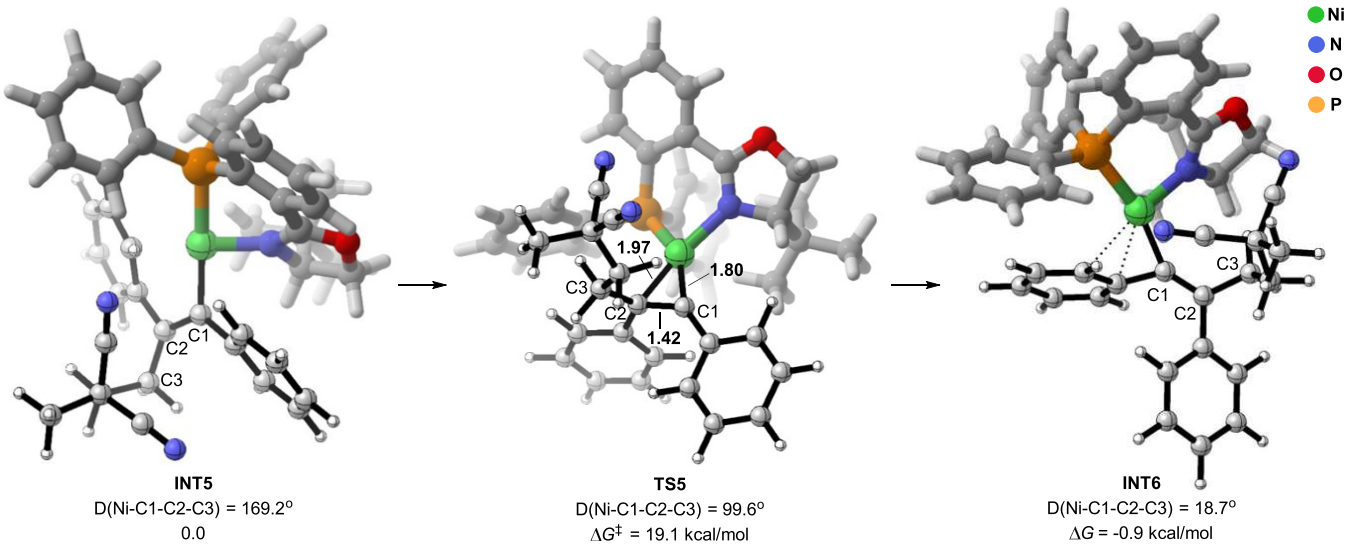

Figure 2. *E*/*Z* isomerization of the alkenylnickel species (distances in Å).

exothermic by 0.9 kcal/mol. In the transition state, alkene coordinates to the nickel with bond lengths of Ni−C1 and Ni−C2 being 1.80 and 1.97 Å, respectively. The dihedral angle of Ni−C1−C2−C3 is 99.6°, showing that substituents on C2 are nearly perpendicular to the Ni−C1−C2 plane (Figure 2).

INT6 from the above-mentioned isomerization process is not saturated in terms of Ni's coordination, and therefore it can then form complexes of **INT7** and **INT8** through CN coordination, releasing Gibbs free energy of about 1−2 kcal/mol. **INT7** and **INT8** are close in energy, and there is an equilibrium between **INT7** and **INT8**, through easy dissociation/coordination of the cyano group to Ni.

Both **INT7** (via **TS7**) and **INT8** (via **TS8**) can undergo CN insertion. The former is more favored than the latter by 1.9 kcal/mol, suggesting that *R* configuration product **3a** is the major product with ee of 92%.[16] The experimentally observed ee is 83%. The reason for this stereochemistry is due to the steric repulsion between the substrate and the ligand. In both **TS7** and **TS8**, the remaining cyano group is located in the pseudo-axial position of the formal six-membered ring (Figure 3). In the energy-favored **TS7**, the cyano group stands underneath the N−Ni−P plane, while cyano group lies above the plane producing more steric repulsion with the *tert*-butyl group of Phox ligand in **TS8**.

Formation of **INT5′** is disfavored kinetically compared to the formation of **INT5**. But **INT5′** is more stable than **INT5** by 9.3 kcal/mol. Therefore, it is possible that, through the rotation of alkene group, **INT5** can isomerize to **INT5′**, which could act as a resting state in the reaction. We can rule out this possibility because the corresponding transition state of rotation, **TS-rot1**, is 1.5 kcal/mol higher than the *Z*/*E* isomerization transition state **TS5** converting **INT5** to **INT6**, which is irreversible due to the ready CN addition afterward. We have also considered the interconversion of **INT5′** and **INT6′**, which is much harder under present conditions with the activation energy of 35.0 kcal/mol. Based on these, the reaction pathway via the orange line in Figure 1 can be ruled out.

Even though **INT6′** is more stable than **INT6**, rotation from **INT6** to **INT6′** requires higher activation energy than the followed step from **INT7** to the product through cyano addition (**TS-rot2**, 17.7 vs 8.3 kcal/mol, detailed in the Supporting Information). Therefore, the pathway via **INT6′** is not favored.

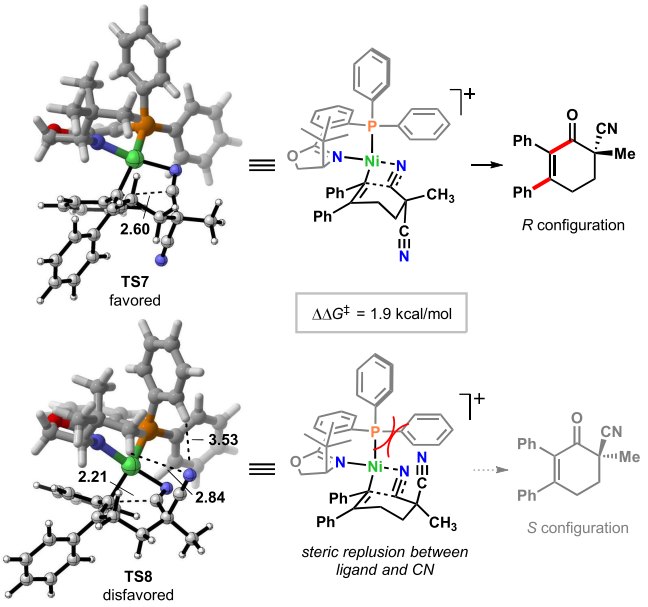

Figure 3. Structures and Gibbs energy difference of **TS7** and **TS8** (distances in Å).

In summary, we have studied the detailed processes of nickel-catalyzed desymmetrizing cascade annulation of alkyne-tethered malononitriles with aryl boronic acids. This reaction starts from water-promoted transmetalation, followed by regioselective alkyne insertion. The ensuing alkenylnickel *E*/*Z* isomerization is the rate-determining step of the catalytic process, which is followed by the stereodetermining step of CN addition, preferring to adopt a six-member-ring transition state with a bystander CN group staying away from the ligand, and giving the final product with *R* configuration. Further development of new reactions guided by this research is ongoing in our laboratories.

https://doi.org/10.1021/acs.joc.2c01269
J. Org. Chem. 2022, 87, 16079−16083

■ ASSOCIATED CONTENT

Supporting Information

The Supporting Information is available free of charge at https://pubs.acs.org/doi/10.1021/acs.joc.2c01269.

More discussions of competing pathways, computational details, and selection of DFT functionals (PDF)

■ AUTHOR INFORMATION

Corresponding Authors

Wen-Bo Liu − *Sauvage Center for Molecular Sciences; Engineering Research Center of Organosilicon Compounds & Materials, Ministry of Education; College of Chemistry and Molecular Sciences, Wuhan University, Wuhan, Hubei 430072, China;* orcid.org/0000-0003-2687-557X; Email: wenboliu@whu.edu.cn

Zhi-Xiang Yu − *Beijing National Laboratory for Molecular Sciences (BNLMS), Key Laboratory of Bioorganic Chemistry and Molecular Engineering of Ministry of Education, College of Chemistry, Peking University, Beijing 100871, China;* orcid.org/0000-0003-0939-9727; Email: yuzx@pku.edu.cn

Authors

Yu-Qing Zheng − *Sauvage Center for Molecular Sciences; Engineering Research Center of Organosilicon Compounds & Materials, Ministry of Education; College of Chemistry and Molecular Sciences, Wuhan University, Wuhan, Hubei 430072, China*

Chen-Long Li − *Beijing National Laboratory for Molecular Sciences (BNLMS), Key Laboratory of Bioorganic Chemistry and Molecular Engineering of Ministry of Education, College of Chemistry, Peking University, Beijing 100871, China*

Complete contact information is available at: https://pubs.acs.org/10.1021/acs.joc.2c01269

Notes

The authors declare no competing financial interest.

■ ACKNOWLEDGMENTS

The numerical calculations in this paper have been done on the supercomputing system in the Supercomputing Center of Wuhan University. This work was supported by the National Natural Science Foundation of China (21933003, 21971198, 22222111).

■ REFERENCES

(1) Selected reviews about all-carbon−quaternary center-containing natural products and drugs: (a) Newman, D. J.; Cragg, G. M. Natural Products as Sources of New Drugs from 1981 to 2014. *J. Nat. Prod.* **2016**, *79*, 629. (b) Ling, T.; Rivas, F. All-carbon quaternary centers in natural products and medicinal chemistry: recent advances. *Tetrahedron* **2016**, *72*, 6729.

(2) Selected reviews about the synthesis of all-carbon−quaternary center-containing natural products: (a) Büschleb, M.; Dorich, S.; Hanessian, S.; Tao, D.; Schenthal, K. B.; Overman, L. E. Synthetic Strategies toward Natural Products Containing Contiguous Stereogenic Quaternary Carbon Atoms. *Angew. Chem., Int. Ed.* **2016**, *55*, 4156. (b) Long, R.; Huang, J.; Gong, J.-X.; Yang, Z. Direct construction of vicinal all-carbon quaternary stereocenters in natural product synthesis. *Nat. Prod. Rep.* **2015**, *32*, 1584. (c) Pritchett, B. P.; Stoltz, B. M. Enantioselective palladium-catalyzed allylic alkylation reactions in the synthesis of *Aspidosperma* and structurally related monoterpene indole alkaloids. *Nat. Prod. Rep.* **2018**, *35*, 559. (d) Li, C.; Ragab, S. S.; Liu, G.; Tang, W. Enantioselective formation of quaternary carbon stereocenters in natural product synthesis: a recent update. *Nat. Prod. Rep.* **2020**, *37*, 276.

(3) Lu, Z.; Hu, X.-D.; Zhang, H.; Zhang, X.-W.; Cai, J.; Usman, M.; Cong, H.; Liu, W.-B. Enantioselective Assembly of Cycloenones with a Nitrile-Containing All-Carbon Quaternary Center from Malononitriles Enabled by Ni Catalysis. *J. Am. Chem. Soc.* **2020**, *142*, 7328.

(4) (a) Hu, X.-D.; Chen, Z.-H.; Zhao, J.; Sun, R.-Z.; Zhang, H.; Qi, X.; Liu, W.-B. Enantioselective Synthesis of α-All-Carbon Quaternary Center-Containing Carbazolones via Amino-palladation/Desymmetrizing Nitrile Addition Cascade. *J. Am. Chem. Soc.* **2021**, *143*, 3734. (b) Zhang, H.; Li, W.; Hu, X.-D.; Liu, W.-B. Enantioselective Synthesis of Fused Isocoumarins via Palladium-Catalyzed Annulation of Alkyne-Tethered Malononitriles. *J. Org. Chem.* **2021**, *86*, 10799.

(5) Cai, J.; Bai, L.-G.; Zhang, Y.; Wang, Z.-K.; Yao, F.; Peng, J.-H.; Yan, W.; Wang, Y.; Zheng, C.; Liu, W.-B. Ni-catalyzed enantioselective [2 + 2 + 2] cycloaddition of malononitriles with alkynes. *Chem.* **2021**, *7*, 799.

(6) Chen, Z.-H.; Sun, R.-Z.; Yao, F.; Hu, X.-D.; Xiang, L.-X.; Cong, H.; Liu, W.-B. Enantioselective Nickel-Catalyzed Reductive Aryl/Alkenyl−Cyano Cyclization Coupling to All-Carbon Quaternary Stereocenters. *J. Am. Chem. Soc.* **2022**, *144*, 4776.

(7) Theoretically experimental and computational studies about transmetalation: (a) Lennox, A. J. J.; Lloyd-Jones, G. C. Transmetalation in the Suzuki−Miyaura Coupling: The Fork in the Trail. *Angew. Chem., Int. Ed.* **2013**, *52*, 7362. (b) Payard, P.-A.; Perego, L. A.; Ciofini, I.; Grimaud, L. Taming Nickel-Catalyzed Suzuki-Miyaura Coupling: A Mechanistic Focus on Boron-to-Nickel Transmetalation. *ACS Catal.* **2018**, *8*, 4812.

(8) Selective examples of base-free Suzuki−Miyaura reaction: (a) Malapit, C. A.; Bour, J. R.; Brigham, C. E.; Sanford, M. S. Base-free nickel-catalysed decarbonylative Suzuki−Miyaura coupling of acid fluorides. *Nature* **2018**, *563*, 100. (b) Zhang, C.; Zhao, R.; Dagnaw, W. M.; Liu, Z.; Lu, Y.; Wang, Z.-X. Density Functional Theory Mechanistic Insight into the Base-Free Nickel-Catalyzed Suzuki−Miyaura Cross-Coupling of Acid Fluoride: Concerted versus Stepwise Transmetalation. *J. Org. Chem.* **2019**, *84*, 13983.

(9) (a) Huggins, J. M.; Bergman, R. G. Reaction of alkynes with a methylnickel complex: observation of a cis insertion mechanism capable of giving kinetically controlled trans products. *J. Am. Chem. Soc.* **1979**, *101*, 4410. (b) Huggins, J. M.; Bergman, R. G. Mechanism, regiochemistry, and stereochemistry of the insertion reaction of alkynes with methyl(2,4-pentanedionato)(triphenylphosphine)nickel. A *cis* insertion that leads to *trans* kinetic products. *J. Am. Chem. Soc.* **1981**, *103*, 3002.

(10) Bottcher, S. E.; Hutchinson, L. E.; Wilger, D. J. Nickel-Catalyzed *anti*-Selective Alkyne Functionalization Reactions. *Synthesis* **2020**, *52*, 2807.

(11) (a) Pawliczek, M.; Schneider, T. F.; Maaß, C.; Stalke, D.; Werz, D. B. Formal *anti*-Carbopalladation Reactions of Non-Activated Alkynes: Requirements, Mechanistic Insights, and Applications. *Mechanistic Insights, and Applications. Angew. Chem. Int. Ed.* **2015**, *54*, 4119. (b) Schitter, T.; Reding, A.; Werz, D. B. Cascades Involving *anti*-Carbopalladation Steps: From Our Initial Hypothesis to Natural Product Synthesis. *Synlett* **2019**, *30*, 1275.

(12) All the structures in the potential energy surface were calculated at the B3LYP-D3(BJ)/def2-TZVP//$SMD_{toluene}$//B3LYP-D3(BJ)/def2-SVP level. More details about the computational method, energies, and geometries are provided in the Supporting Information. B3LYP-D3(BJ) has been found efficient and popular for studying the mechanism of nickel-catalyzed reactions: Sperger, T.; Sanhueza, I. A.; Kalvet, I.; Schoenebeck, F. Computational Studies of Synthetically Relevant Homogeneous Organometallic Catalysis Involving Ni, Pd, Ir, and Rh: An Overview of Commonly Employed DFT Methods and Mechanistic Insights. *Chem. Rev.* **2015**, *115*, 9532.

(13) For selected recent computational studies of Ni-catalyzed reactions, see: (a) Huang, Y.; Ma, C.; Liu, S.; Yang, L.-C.; Lan, Y.; Zhao, Y. Ligand coordination- and dissociation-induced divergent allylic alkylations using alkynes. *Chem.* **2021**, *7*, 812. (b) Yao, W.-W.;

Li, R.; Chen, H.; Chen, M.-K.; Luan, Y.-X.; Wang, Y.; Yu, Z.-X.; Ye, M. Ni-catalyzed hydroaminoalkylation of alkynes with amines. *Nat. Commun.* **2021**, *12*, 3800. (c) Tambe, S. D.; Ka, C. H.; Hwang, H. S.; Bae, J.; Iqbal, N.; Cho, E. J. Nickel-Catalyzed Enantioselective Synthesis of 2,3,4-Trisubstituted 3-Pyrrolines. *Angew. Chem., Int. Ed.* **2022**, *61*, e202203494. (d) Choi, H.; Lyu, X.; Kim, D.; Seo, S.; Chang, S. *Endo*-Selective Intramolecular Alkyne Hydroamidation Enabled by NiH Catalysis Incorporating Alkenylnickel Isomerization. *J. Am. Chem. Soc.* **2022**, *144*, 10064.

(14) **INT1** could form a more stable complex with either substrate, solvent, or product, and this complex could be the resting state of the reaction, which was not investigated here. From this species of resting state to **INT1** could be the rate-determining step if this is more difficult than the isomerization process discussed later on.

(15) Crabtree, R. H. *The Organometallic Chemistry of the Transition Metals*, 6th ed.; Wiley, 2014; p 9.

(16) Theoretical enantiomeric excess was calculated using Eyring equation under 298 K.

https://doi.org/10.1021/acs.joc.2c01269
J. Org. Chem. 2022, 87, 16079−16083